THE GEOLOGICAL SOCIETY OF AMERICA®

Technical Note

A Simple Method for Measuring Discontinuity Orientations from Terrestrial LIDAR Data

NORBERT H. MAERZ[1]

Geological Engineering Program, Missouri University of Science and Technology, 1006 Kingshighway, Rolla, MO 65409-0660

AHMED M. YOUSSEF

Geological Hazards Department, Saudi Geological Survey, P.O. Box 54141, Jeddah 21514, Saudi Arabia

JAMES N. OTOO

TRAVIS J. KASSEBAUM

Geological Engineering Program, Missouri University of Science and Technology, 1006 Kingshighway, Rolla, MO 65409-0660

YE DUAN

Department of Computer Science, University of Missouri–Columbia, 209 Engineering Building W, Columbia, MO 65211

Key Terms: ***Terrestrial LiDAR, Discontinuities, Orientation, Measurement, Three-Point Problem***

INTRODUCTION

The measurement of discontinuity (joint) orientations is critical in assessing the stability of discontinuous rock slopes. The discontinuity orientations are used as input to all discontinuous modeling programs and methods, including kinematic screening methods and limited equilibrium sliding methods.

Manual Discontinuity Measurements

Traditionally, discontinuity orientations are measured manually using a compass (Figure 1). The drawbacks of this method include the fact that these measurements are slow, are tedious, often subject the user to physical danger (from rock falls and/or the need to scale slopes for measurements at heights), and may be inaccurate due to sampling biases when measurements are restricted to accessible areas only.

LiDAR Measurements

Terrestrial LiDAR (light detection and ranging) scanners (Figure 2) can return detailed three-dimensional (3-D) maps or point clouds of rock slopes. These include highly accurate maps of planar features such as joints and other discontinuities. Joint orientations can be measured on these point clouds in various ways. LiDAR scanners are increasingly being used for the purpose of measuring discontinuity orientations (Bulut and Tüdes, 1996; Feng, 2001; Post, 2001; Donovan et al., 2005; Strouth and Eberhard, 2006; Haneberg, 2008; Olariu et al., 2008; Lato et al., 2009; Sturzeinegger and Stead, 2009; Gigli and Casagli, 2011; and Otoo et al., 2011).

Systematic LiDAR Orientation Measurements

One way to automatically generate orientations from LiDAR scans is to use advanced algorithms to create solid models (polygonal models) where each polygon represents a planar face. The typical LiDAR measurements work well in general when using scans from vegetation-free continuous rock cuts or slopes where the exposure is entirely composed of discontinuity surfaces. Where vegetation is present, or blast- or weathering-created fractures are encountered, the automated algorithms need sophisticated filters or human interpretation to classify which rock surfaces are discontinuities that should be measured.

These algorithms automatically extract planar features (discontinuities) from the scan, calculate orientations, cluster the orientations, and present them on a stereonet. Typically, LiDAR methods require survey

[1]Corresponding author, tel: 573 341-6714, fax: 573 341-4368, email: norbert@mst.edu.

Figure 1. Manual measurements of joints are slow, tedious, expose the user to danger, and are often limited to locations that are easily accessible.

control to tie the LiDAR to the true north grid. The drawbacks of this method are that it requires continuously exposed rock throughout the scanned images, and sophisticated algorithms that are frequently incapable of distinguishing between discontinuities like joints as opposed to other planar elements such as blast-induced fractures or erosional surfaces.

Spot LiDAR Orientation Measurements

This paper describes an alternative approach that allows the geologist or engineer to select individual discontinuities from a point cloud by browsing through the point cloud in a viewer, selecting discontinuities to be measured, and then calculating the discontinuity orientation using the so-called "three-point" method, which can be programmed into a spreadsheet. In addition, the method does not require any surveying; it simply calibrates using a single manual orientation measurement. This approach is very simple, because it requires only a LiDAR viewer to "pick" points on the point cloud and a spreadsheet to do the calculations.

METHODOLOGY

LiDAR Scans

LiDAR scans are taken using a suitable scanner; this research used a Leica ScanStation II scanner (Figure 2). Figure 4 shows an example of scanning difficult-to-reach areas. For the purpose of measuring discontinuities, scanning resolution (point density) does not need to be set very high; typically about 5 cm horizontal and vertical resolution is sufficient to measure

Figure 2. Leica ScanStation II in Saudi Arabia.

discontinuities. Scanning time with a ScanStation II at this resolution on a typical slope or cut is less than 2 minutes. Optical imaging is done beforehand, so that the points in the point cloud can be highlighted with the optical color most closely associated with each point. This allows the user to more easily identify joint surfaces when browsing through the point cloud image in the LiDAR viewer. No survey control is required in this method, further saving time in the field.

Manual Measurements

A single manual orientation (calibration) measurement on any sub-vertical planar feature must be undertaken in this methodology. If a sub-vertical discontinuity is not present, any planar structure like a wide board can be placed in the field of view. Any number of manual (verification) measurements on discontinuities in the scanning image may be added.

Calibration Measurement

The LiDAR point cloud is defined by a set of (x,y,z) coordinates. The z (vertical) coordinates are

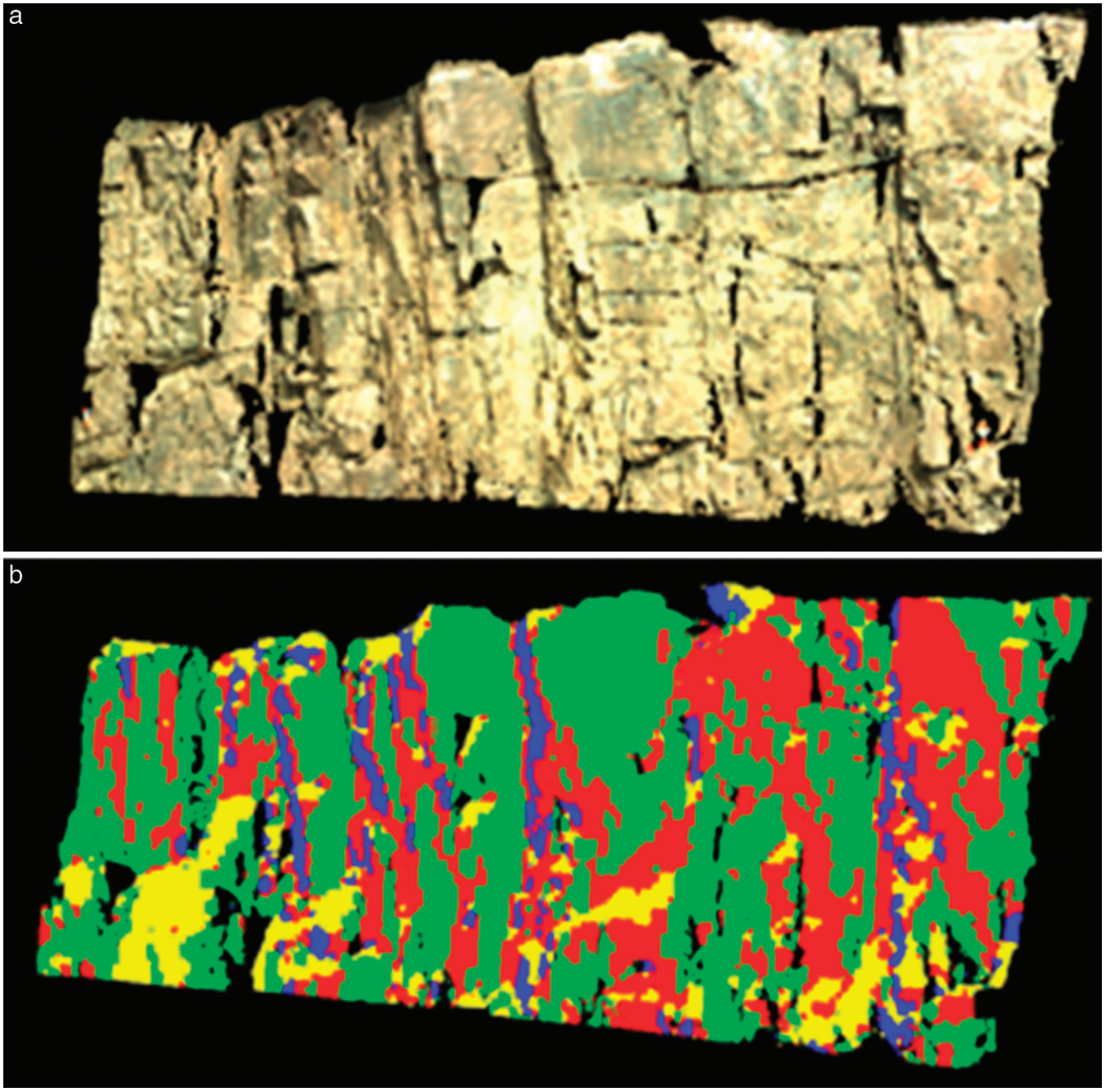

Figure 3. (A) LiDAR scan of a Missouri ignimbrite rock cut. This point cloud was generated with a Leica ScanStation II, which incorporates optical imaging and allows each point in the point cloud to be painted by its corresponding optical color. (B) Automatic identification of discontinuity orientations; the different colors are assigned to discontinuities of similar orientations based on cluster analysis. Green color represents mean orientation of 88/186, blue represents mean orientation of 89/277, yellow represents mean orientation of 37/338, and red represents mean orientation of 82/203.

inherently correct as the z-axis is always vertical, provided that the LiDAR scanner is correctly leveled. The x- and y-axes are arbitrarily oriented and represent the local coordinate system of the LiDAR scanner. Matching the LiDAR local coordinate systems to a global geographic coordinate system involves survey techniques that, in addition to requiring additional personnel and surveying equipment, increase the time required for measurements.

In this paper, the discontinuity orientations are measured in the local coordinate system, and the measurements are reoriented later. The required control measurements may be obtained easily with a Brunton compass by measuring the orientation of a

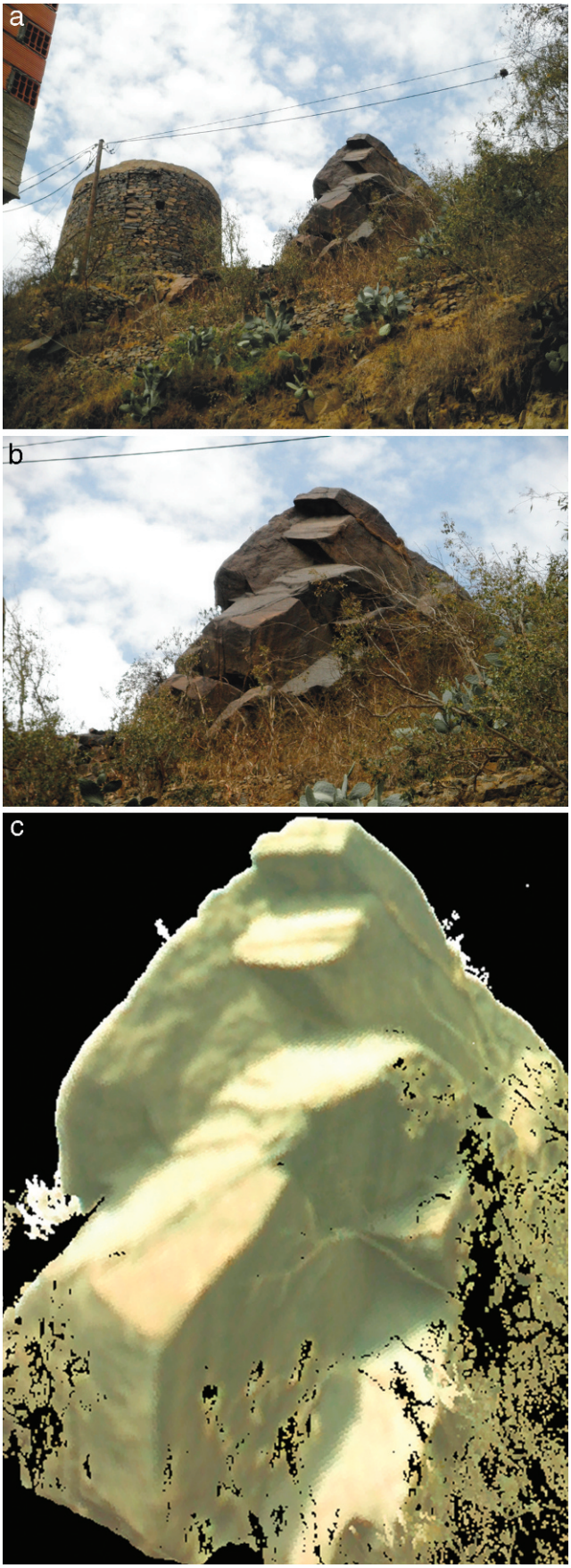

single sub-vertical discontinuity (or any planar structure or target) that appears anywhere in the LiDAR scan and comparing the LiDAR-measured orientation to the manually obtained one. This requires the sub-vertical planar structure to be imaged in the LiDAR scan, and its description/location and its orientation to be accurately recorded in a field notebook. Only one single structure has to be measured both manually and from the LiDAR scan to do this calibration. Magnetic declination must be used to return to "true" north.

Verification Measurements

Optionally, more joints can be measured manually in the field, if verification of LiDAR measurements is desired. Typically, in this case, only the joints that are easily accessible will be manually measured and compared to the LiDAR measurements. As before, it is necessary that the location and measurements of the joints be recorded in a field notebook.

Picking the Three Points for Each Joint on the Point Cloud

Using the LiDAR viewer, three individual points on each joint to be measured are "picked" using the mouse cursor (Figure 5). These points should be spread out as far as possible on the same joint, and care must be taken that the three points are not collinear or close to being collinear. Some LiDAR viewers will allow the coordinates of the data points to be exported, while other LiDAR viewers will require x,y,z values to be manually recorded. In each case, as many significant digits as possible should be retained. It is not possible *a priori* to determine the precision required, but especially in the case of low-angle joints, the dip direction accuracy is sensitive to the number of significant digits in the coordinate values.

Data Calculations

Calculation of the Equation of a Plan (Local Coordinate System)

Given three co-planar (but not collinear) points on a planar surface in a local (arbitrary) coordinate space defined by the LiDAR unit

$$(x1,y1,z1),\ (x2,y2,z2),\ (x3,y3,z3),$$

←

Figure 4. Left (top and bottom): Example of joints in difficult-to-reach places. Right: LiDAR scan of the joints.

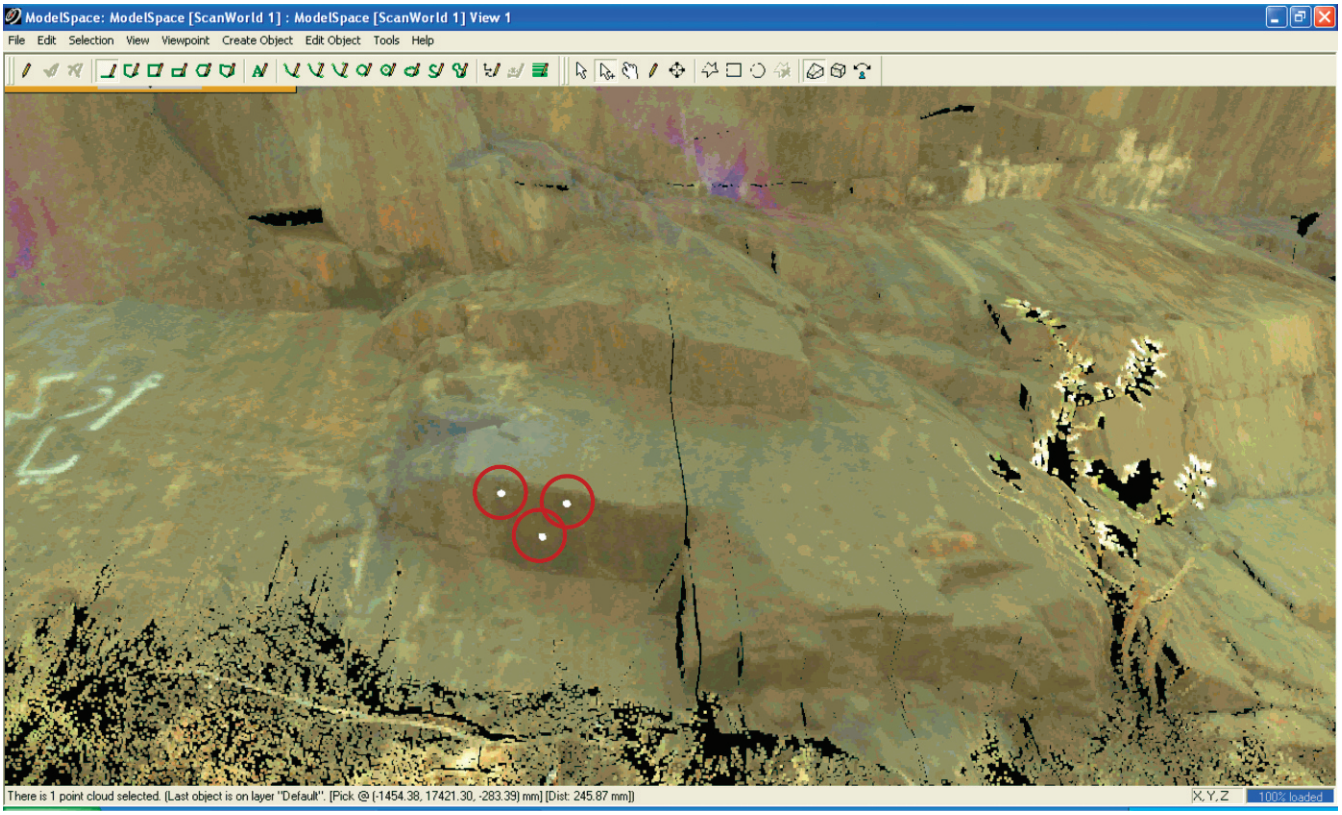

Figure 5. Picking three points off a joint in the Leica LiDAR viewer (highlighted with red circles). Point coordinates of each point as they are selected are displayed in the status bar at the bottom of the image for this particular LiDAR viewer.

the equation of a plane is defined as:

$$Ax+By+Cz+D=0$$

(Grossman, 1981), where (A,B,C) is a vector normal to the plane. The values of A, B, C, and D are determined as follows:

$$A=y1(z2-z3)+y2(z3-z1)+y3(z1-z2)$$

$$B=z1(x2-x3)+z2(x3-y1)+z3(x1-y2)$$

$$C=x1(y2-y3)+x2(y3-y1)+x3(y1-y2)$$

$$-D=x1(y2z3-y3z2)+x2(y3z1-y1z3)+x3(y1z2-y2z1).$$

(A,B,C) is then converted to a unit-normal vector:

$$(x,y,z)=(A,B,C)/\sqrt{(A^2+B^2+C^2)}.$$

Note that "D" is not required for this calculation.

Conversion from Cartesian to Spherical Coordinates (Local Coordinate System)

Cartesian coordinates (x,y,z) of the unit-normal vector are then converted to spherical coordinates (r,θ,φ) (radius, inclination, azimuth) (Figure 6). Note that since we are concerned with unit normals on the unit hemisphere, r will always be equal to 1, so it need not be calculated.

The values of φ and θ (in radians) are calculated as

$$\cos\theta=z/r \text{ (where } r=1)$$

and

$$\cos\varphi=x/\sqrt{(x^2+y^2)}.$$

Rectification of φ Value (Local Coordinate System)

The value of φ as determined in the previous section will always result in a value between 0 and π/2 (0 and 180 degrees), whereas the geographical coordinate system requires a value between 0 and 2π (0 and 360 degrees) in a clockwise direction (Figure 7).

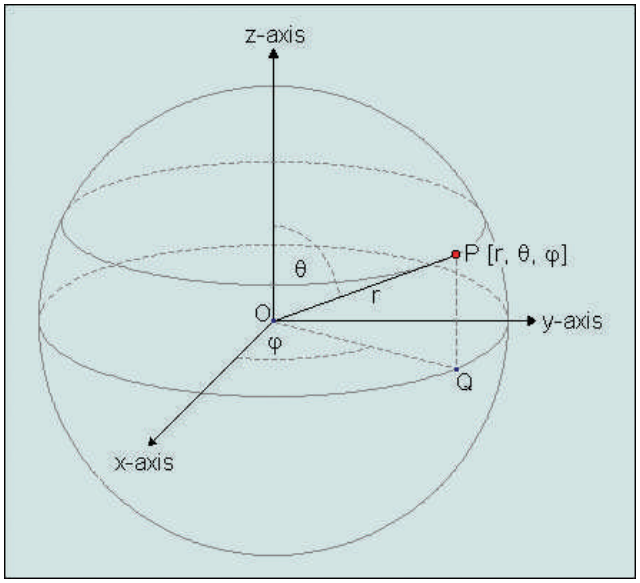

Figure 6. Spherical coordinate system (http://www.vias.org/comp_geometry/math_coord_sphere.htm).

The transformation is as follows (quadrants as defined in Figure 7):

If in quadrant 1 ($x>0$, $y<0$) $\varphi \rightarrow 90-\varphi$.

If in quadrant 2 ($x<0$, $y<0$) $\varphi \rightarrow 90+\varphi$.

If in quadrant 3 ($x<0$, $y>0$) $\varphi \rightarrow 90+\varphi$.

If in quadrant 4 ($x>0$, $y>0$) $\varphi \rightarrow 450-\varphi$.

Rotation of φ Value (Local Coordinate System to Global)

The φ angle is then aligned (rotated) from the local coordinate system to a global coordinate system (with north as the reference for the y-axis) (Figure 8). This is simply done empirically, by manually measuring a single discontinuity in the field using a compass and comparing the φ value measured in the field with the φ value measured on the LiDAR image. The difference in degrees between the two is simply measured, and then that difference is added to all orientations measured in the local coordinate system.

FIELD VERIFICATION MEASUREMENTS

Rolla, MO

Two local sites were selected in a small local sandstone rock cut to verify the method. Appendix 1 shows the results of comparing manual and LiDAR-derived discontinuity orientation measurements. Results are presented in the form of stereonets. Each scan took about 45 minutes in the field, including setup. Picking the points on the LiDAR image and generating the orientation data took about 60 to 90 minutes.

Ironton County, MO

A single site was selected in an ignimbrite rock cut to verify the measurements (Appendix 2).

Fayfa Mountains, Saudi Arabia

LiDAR scans were made on four sites of phyllite, diorite, syenite, and amphibolites in the Fayfa Mountains in southeastern Saudi Arabia (Appendix 3). Measurements of a few discontinuity orientations were made from the LiDAR scans and calibrated and corroborated with several manual measurements. Additional LiDAR measurements were made on discontinuities that were not easily accessible.

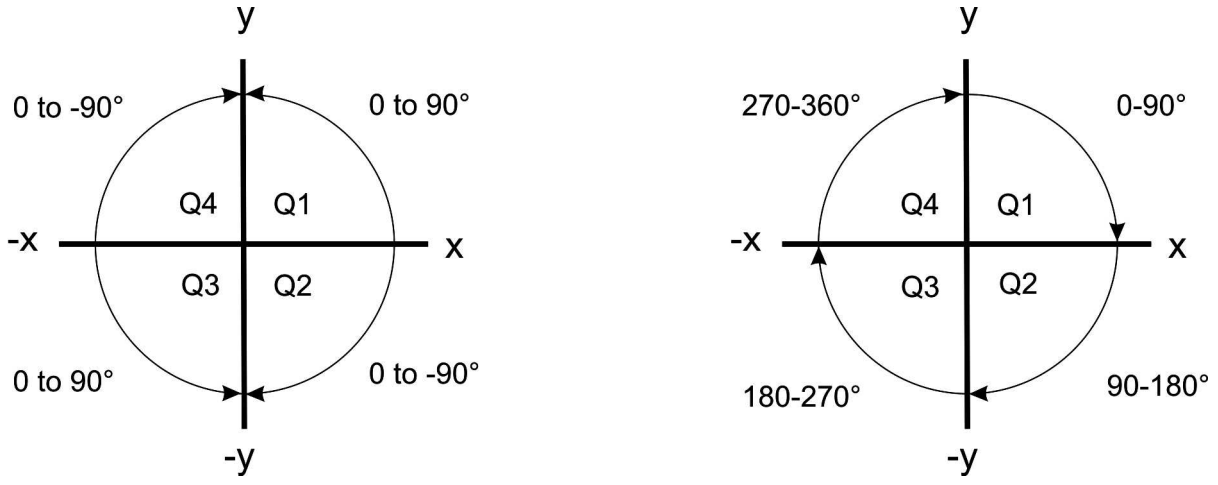

Figure 7. Left: Spherical coordinate system φ angles. Right: Un-aligned global φ angles. Q1= Quadrant 1.

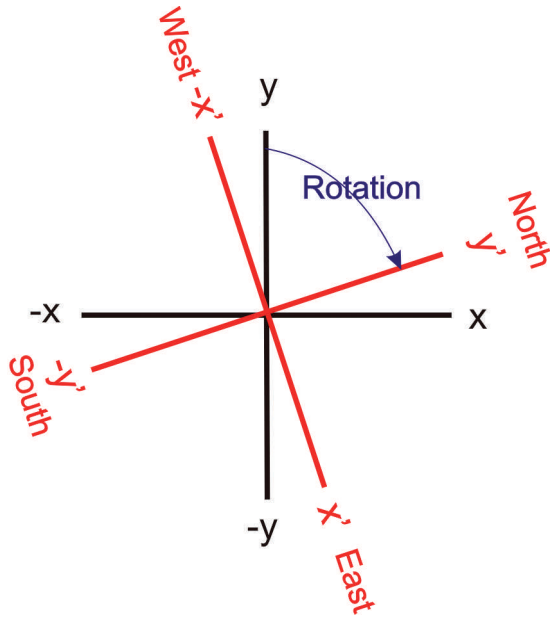

Figure 8. The rotation angle is the difference between the global coordinate system defined by north (in red) and the arbitrary LiDAR local coordinate system in which the LiDAR measurements are taken (in black).

CONCLUSION

The results of this investigation show how quickly, easily, and accurately joint orientation data can be obtained from LiDAR scans, avoiding manual measurements that are both time consuming, incomplete, and dangerous. In addition, LiDAR can give us virtual accessibility to measure discontinuities at locations that cannot easily be accessed for manual measurements.

Comparison of the orientation results shows that the manually (compass) measured results are fairly close to the LiDAR measurements. Differences are likely to be caused by the fact that typically discontinuities are not perfectly planar, and variable measurements can be expected depending on the part of the discontinuity on which the measurements are made, and the base length over which the discontinuity is assumed to be planar. For a full discussion about these errors, please see Fecker and Rengers (1971), where discontinuity orientations were measured on flat plates of different sizes pressed onto the discontinuity surface.

ACKNOWLEDGMENTS

The authors would like to acknowledge the National Science Foundation grant number 0856420 for sponsorship of the U.S. portion of the work, and the Saudi Geological Survey for supporting the fieldwork in Saudi Arabia, and we wish to express our sincere appreciation to the Saudi Geological Survey personnel, specifically, Mr. Saleh Sefry, the director of the Applied Geology Division, Mr. Hassan Al-Harbi, the head of the Geological Hazard Department, and Mr. Abdullah Otabi and Mr. Saaid Al-Zahrani for their support and assistance during the time of the project.

REFERENCES

Bulut, F. and Tüdes, S., 1996, Determination of discontinuity traces on inaccessible rock slopes using electronic tacheometer: An example from the Ikizdere (Rize) region, Turkey: *Engineering Geology*, Vol. 44, pp. 229–233.

Donovan, J.; Kemeny, J.; and Handy, J., 2005, The application of three-dimensional imaging to rock discontinuity characterization. In *Alaska Rocks, Proceedings of the 40th U.S. Rock Mechanics Symposium*, Anchorage, AK, June 25–29, 2005: 7 p.

Fecker, E. and Rengers, N., 1971, Measurement of large scale roughness of rock planes by means of profilograph and geological compass. In *Proceedings of the International Symposium on Rock Fracture*: International Society for Rock Mechanics, Nancy, France, pp. 1–18.

Feng, Q., 2001, *Novel Methods for 3-D Semi-Automatic Mapping of Fracture Geometry at Exposed Rock Faces*: Ph.D. Thesis, Division of Engineering Geology, Royal Institute of Technology (KTH), Stockholm, Sweden.

Gigli, G. and Casagli, N., 2011, Semi-automatic extraction of rock mass structural data from high resolution LiDAR point clouds: *International Journal of Rock Mechanics and Mining Sciences*, Vol. 48, No. 2, pp. 187–198.

Grossman, S., 1981, *Calculus,* 2nd ed: Academic Press, New York, 1019 p.

Haneberg, W., 2008, Using close range terrestrial digital photogrammetry for 3-D rock slope modeling and discontinuity mapping in the United States: *Bulletin of Engineering Geology and the Environment*, Vol. 67, No. 4, pp. 457–469.

Lato, M.; Hutchinson, J.; Diederichs, M.; Ball, D.; and Harrap, R., 2009, Engineering monitoring of rockfall hazards along transportation corridors: Using mobile terrestrial LiDAR: *Natural Hazards and Earth System Sciences*, Vol. 9, pp. 935–946.

Olariu, M. I.; Ferguson, J. F.; and Aiken, C. L., 2008, Outcrop fracture characterization using terrestrial laser scanners: Deep-water Jackfork sandstone at Big Rock Quarry, Arkansas: *Geosphere*, Vol. 4, No. 1, pp. 247–259.

Otoo, J. N.; Maerz, N. H.; Xiaoling, L.; and Duan, Y., 2011, 3-D discontinuity orientations using combined optical imaging and LiDAR techniques. In *Proceedings of the 45th U.S. Rock Mechanics Symposium*, San Francisco, CA, June 26–29, 2011: 9 p.

Post, R., 2001, *Characterizing of Joints and Fractures in a Rock Mass Using Digital Image Processing*: M.S. Thesis, University of Arizona, Tucson, AZ, 105 p.

Strouth, A. and Eberhard, E., 2006, The use of LiDAR to overcome rock slope hazard data collection challenges at Afternoon Creek, Washington. In *Methods for Rock Face Characterization workshop*, Golden, CO, June 17–21, 2006: pp. 49–62.

Sturzeinegger, M. and Stead, D., 2009, Close-range terrestrial digital photogrammetry and terrestrial laser scanning for discontinuity characterization on rock cuts: *Engineering Geology*, Vol. 106, pp. 163–182.

APPENDIX 1: MEASUREMENTS IN ROLLA, MO

Figure A1-1. Rolla site A.

Table A1-1. *Discontinuity orientation measurements (dip direction/dip angle) from LiDAR measurements compared to manual measurement.*

Dip Direction / Dip Angle in Degrees	
Field	LIDAR
314/86	309/88
332/70	329/67
022/88	022/87
310/83	314/84
333/80	339/78
322/75	328/71
035/87	031/89
298/86	302/80
355/01	358/01
177/85	172/82
174/78	182/78
274/01	274/02
026/45	023/45
182/74	188/73
191/75	191/79
355/76	355/76
353/72	359/75
350/70	353/67
035/89	037/88
003/89	008/83

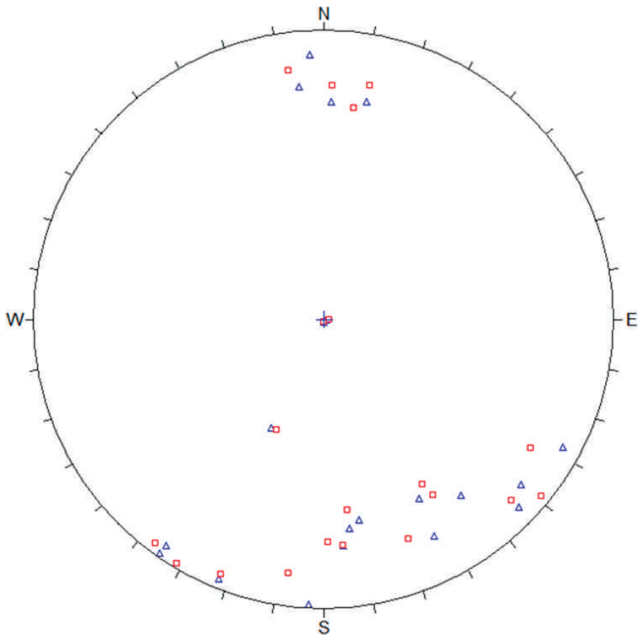

Figure A1-2. Equal-angle lower-hemisphere projection. Points are plotted as poles. Blue triangles are manual measured discontinuities; red squares are LiDAR-generated measurements.

APPENDIX 2: MEASUREMENTS IN IRONTON COUNTY, MO

Figure A2-1. Ironton County site.

Table A2-1. *Discontinuity orientation measurements (dip direction/dip angle) from LiDAR measurements compared to manual measurement.*

Dip Direction / Dip Angle in Degrees	
Field	LIDAR
008/51	011/54
108/85	112/87
006/07	008/09
198/63	200/65
159/85	162/87
102/87	105/86
158/78	156/77
101/82	112/88
021/47	023/48
218/61	215/60

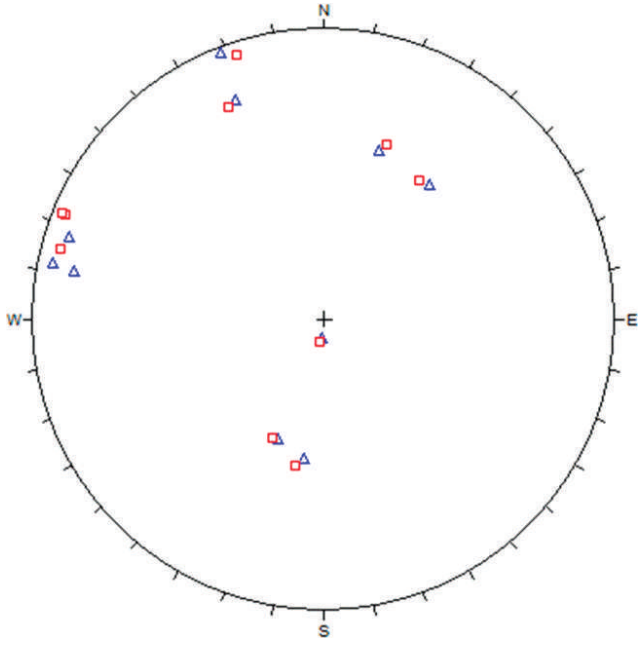

Figure A2-2. Equal-angle lower-hemisphere projection. Points are plotted as poles. Blue triangles are manual measured discontinuities; red squares are LiDAR-generated measurements.

APPENDIX 3: MEASUREMENTS IN FAYFA MOUNTAINS, SAUDI ARABIA

Figure A3-1. Site S24.2.

Table A3-1. *Discontinuity orientation measurements (dip direction/dip angle) from LiDAR measurements compared to manual measurement.*

Dip Direction / Dip Angle in Degrees	
Field	LIDAR
004/80	004/83
096/89	098/88
144/50	149/60
	150/56
	330/22
	144/70
	107/86
	291/77
	168/45
	011/52
150/52	150/56
	244/13
	348/29
	271/81

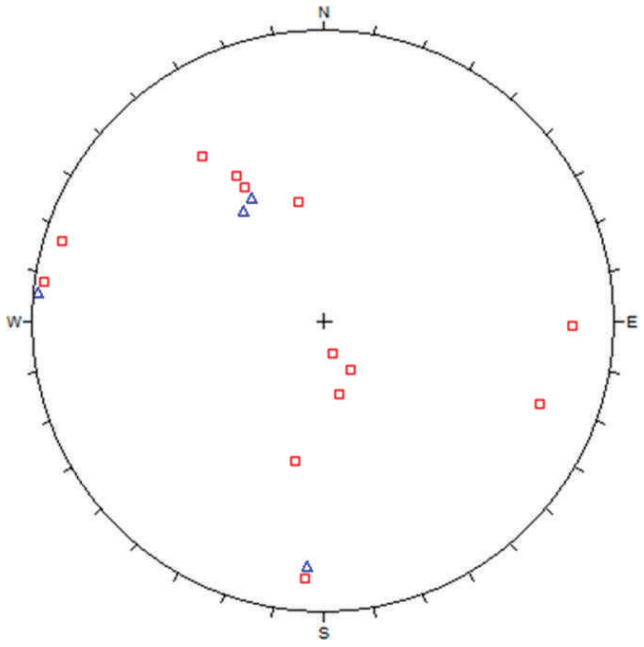

Figure A3-2. Equal-angle lower-hemisphere projection. Points are plotted as poles. Blue triangles are manual measured discontinuities; red squares are LiDAR-generated measurements.